ELSEVIER

Journal of Materials Processing Technology 172 (2006) 249–257

Journal of Materials Processing Technology

www.elsevier.com/locate/jmatprotec

Distortion minimization during gas quenching process

Zhichao Li, Ramana V. Grandhi *, Raghavan Srinivasan

Department of Mechanical and Material Engineering, Wright State University, Dayton, OH 45435, USA

Received 20 November 2001; received in revised form 6 March 2002; accepted 5 October 2005

Abstract

During gas quenching, independent process parameters include the preheat temperature of the component and the temperature of the circulated gas. One of the most important dependent process parameters is the heat transfer coefficient between the component and the circulated gas. The heat transfer coefficient has significant influence on the quenching results, such as distortion, residual stresses, and hardness distribution. Large distortions after quenching will increase the cost due to the post-quenching processes, such as the grinding and hot rectification. The objective in this research is to minimize the distortion caused by quenching. In this paper, the surface of a component is divided into several regions, and different values of the heat transfer coefficient are imposed on each region. Constraints on the residual stresses and surface hardness distribution are imposed to improve the service properties. The heat transfer coefficients are ideal design variables to optimize the gas quenching process. The commercial finite element software, DEFORM-HT, is used to predict the material response during the quenching process. The response surface method is used to obtain the analytical models of the objective function and constraints in terms of the design variables. Once the closed-form response surface models are obtained, a commercially available design optimization tool, design optimization tool (DOT), is used to search for the optimum design point. This paper summarizes the methodology used to optimize the gas quenching process together with an application of a steel disk example.
© 2005 Elsevier B.V. All rights reserved.

Keywords: Distortion; Gas quenching process; Distortion minimization

1. Introduction

Heat treatment of steels involves heating and cooling of the workpiece to obtain the desired physical and mechanical properties. Quenching is an important heat treatment process used to increase the hardness and strength of steel by the martensitic phase transformation. The quenching process can be classified as liquid quenching and gas quenching according to the type of the quenching medium used. In recent years, gas quenching has become more popular in industry with the development of high-pressure furnaces and efficient quenching media [1–3], such as a mixture of nitrogen and helium. Gas quenching has several advantages over the conventional liquid quenching systems [4], and they are listed as follows:

- The rate of heat transfer between the surface of the component and the circulated gas has a large range of flexibility. By increasing the furnace pressure, the gas flow speed, and using nozzles at different surface locations of the component, many steel components can be full hardened by gas quenching that were formerly oil quenched.
- The cooling rate can be controlled more uniformly to minimize the distortion. By adjusting the previously stated parameters, the heat transfer coefficient between the surface of the component and the circulated gas can be well controlled.
- With the use of inert gas, gas quenched components are clean and scale-free.
- Gas quenching is more environmentally friendly than the liquid quenching processes.

Various mathematical models, with different accuracy and complexity, have been developed in the past two decades. There are three general types of models used in the property prediction and computer simulation [5]: static models, dynamic models, and programs with both static and dynamic models. Static models are based on simple empirical formulas derived from experimental data and regression analysis. Dynamic models are based on the solution of a series of differential equations. An important category of dynamic models is the use of the finite element analysis to predict the distortion, residual stresses, and hardness

* Corresponding author.
E-mail address: ramana.grandhi@wright.edu (R.V. Grandhi).

0924-0136/$ – see front matter © 2005 Elsevier B.V. All rights reserved.
doi:10.1016/j.jmatprotec.2005.10.018

distribution [6–11]. The finite element simulation of the quenching process includes the heat transfer, phase transformations, and deformation. These three parts are influenced by each other and should be coupled together during the simulation process.

During heat treatment, process parameters influence the quality of the heat-treated products. Experimental database can be used to design the heat treatment process. For example, the Jominy end-quench experimental data can be used to direct the quenching process design. However, the use of the experimental data is limited due to the limitations of the available experimental database in the handbook. In industry, the trial and error method is still widely used to determine the process parameters during heat treatment. The trial and error method has drawbacks of being costly and time consuming. Furthermore, it cannot provide the optimum design. These drawbacks make the optimization of the heat treatment processes based on computer simulation more important. Two main optimization schemes are used to optimize the heat treatment processes. The first scheme is based on the sensitivity information, which can be calculated by the finite difference method or analytical methods. The other scheme uses the approximation method, such as the response surface method. Röhl and Srivatsa [12] optimized a fan cooling quenching process of a Ni-based superalloy turbine engine disk. In their study, the design variables were the heat transfer coefficients along the surface of the component. The objective function was formulated as a quadratic polynomial that penalizes the deviation from the desired cooling rate. Two constraints were imposed. The first constraint was defined as the average difference between the desired and obtained cooling rates. The second constraint was defined as the difference between the desired and minimum cooling rates. The finite difference method was used to obtain the sensitivity information, and the modified method of feasible directions was used as the optimization scheme. When simulating the heat treatment processes, it is clear that the calculated results are only as good as the data used in the model. Batista and Kosel [13] investigated the influence of the estimated error of input material data on the error of the calculated residual stresses. For this purpose, the mathematical model of the heat treatment process was developed. The sensitivities of the relative error of the calculated residual stresses with different input data were calculated by numerical differentiation. Karthikeyan et al. [14] developed mathematical models to optimize the heat treatment conditions for maximum yield strength and ductility of aluminum–silicon carbide particulate composites. The response surface method was used to fit the mathematical models, and the process variables included the volume fraction of SiC, aging temperature, aging time, and solutionizing time. Saigal and Leisk [15] optimized the tensile properties of alumina/aluminum metal matrix composites using the Taguchi analysis. The process variables taken into consideration were the volume fraction of reinforcement particles, solutionizing time, aging time, and aging temperature. The results indicate that, on average, a 4% increase in the yield strength and a 7% increase in ultimate tensile strength were obtained.

In this paper, the heat transfer coefficients at different locations on the component surface are used as the design variables to optimize the gas quenching process. The finite element analysis of the gas quenching process is implemented by using DEFORM-HT [16]. The objective function is to minimize the distortion of the as-quenched component. Three constraints are imposed on the residual stress and surface hardness distribution to improve the service properties of the component. Quadratic response surface models are used to build the relations of the objective and constraint functions in terms of the design variables. The closed-form response surface models are used to do the optimization instead of conducting several finite element simulations. A commercial design optimization tool, DOT [17], is used to search for an optimum design point. This optimization scheme is demonstrated with a gas quenching process of a disk component.

2. Computational model

The computer simulation of the quenching process includes three main parts: heat transfer; phase transformations; and deformation due to temperature and phase changes. The three parts are influenced by each other during the quenching process, as shown in Fig. 1. The phase transformations are temperature dependent. On the other hand, the latent heat generated by the phase transformations will influence the temperature distribution. The thermal gradient due to heat transfer is one of the main reasons of the stress generation and deformation. The volume change due to phase transformations is another reason of distortion. For most carbon and alloy steels, the martensitic phase transformation has more contribution on the stress generation than the thermal gradients during the quenching process. The heat generated by the plastic deformation is comparatively insignificant than the latent heat due to phase transformations. The influence of stress on the phase transformation, and the heat generated by plastic deformation are neglected in this paper. Basic formulations used for modeling and simulation are introduced.

2.1. Heat transfer

The heat transfer during the gas quenching process is a transient problem. The temperature distribution is governed by

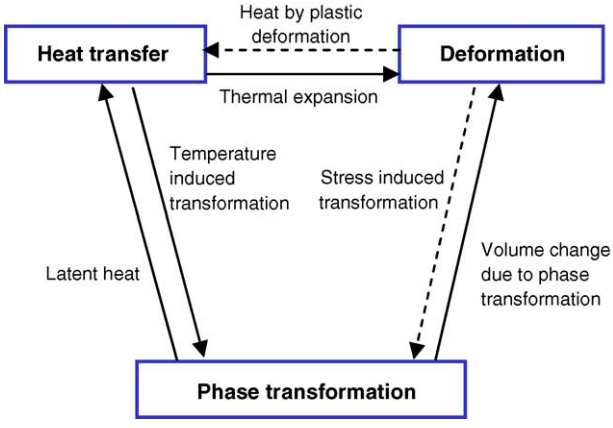

Fig. 1. Coupling between heat transfer, deformation, and phase transformations during the quenching process.

Fourier's formula, which is shown in Eq. (1).

$$\rho c \frac{\partial T}{\partial t} = \frac{\partial}{\partial X}\left(K \frac{\partial T}{\partial X}\right) - \sigma_{ij}\dot{\varepsilon}_{ij}^{p} + L_I \dot{\xi}_I \quad (1)$$

where ρ is the density, c the heat capacity, K the heat conduction coefficient, L_I is the latent heat due to phase transformation, σ_{ij} the stress, $\dot{\varepsilon}_{ij}^{p}$ the plastic strain rate, and ξ_I the volume fraction of the I-th phase transformed. The second and third terms of the right side of the equation represent the heat due to plastic deformation, and latent heat due to phase transformations, respectively.

The rate of heat transmission by convection and radiation between the surface of the solid component and the fluid gas is calculated using the Newton's equation of cooling.

$$Q = hA\,\Delta T \quad (2)$$

where Q is the heat flux, A the surface area of the solid component, ΔT the temperature difference between the surface of the component and the fluid gas, and h the heat transfer coefficient which combines the influences of the convection and radiation. According to its physical meaning, the combined heat transfer coefficient is influenced by the surface temperature of the component. The current and future vacuum heat treating equipment designs demand for the features of faster quench-rate capacity, more precise process cycle and temperature uniformity control [18]. The heat transfer coefficient schedule can be calculated according to the cooling history by the trial and error method, or the inverse techniques [19]. It is possible and necessary to obtain the desired heat transfer coefficient with the new developed gas quenching equipment in industry.

The traditional liquid quenching offers very little room to control the heat transfer. Comparatively, the heat transfer is much easier to control during the gas quenching process. Different mathematical models can be used to represent the heat transfer coefficient. In our previous research work [20], the heat transfer coefficient was modeled as a step function in terms of the quenching time, and a single value is used for the whole component surface. Based on the irregular geometry of the component, different values of the heat transfer coefficient could be imposed on different surface regions to obtain a more uniform surface hardness and to minimize the distortion. In this paper, the heat transfer coefficients vary along the surface of the component, and the value do not change with temperature. The values of the heat transfer coefficients on the different surface regions of the component are used as design variables to optimize the gas quenching process.

2.2. Phase transformation models

Phase transformations during the quenching process have an extensive rearrangement of atoms. Depending on whether diffusion occurs or not, the phase transformations during quenching can be classified as diffusional and martensitic phase transformations. The diffusional phase transformation involves diffusion of carbon and other solute atoms, and it is time dependent. The martensitic phase transformation is diffusionless and occurs very rapidly.

The diffusional phase transformation includes the transformations from austenite to ferrite and cementite. The Johnson–Mehl–(JMA) equation [21] is used to predict the volume fraction of phases transformed in this case, which is given in Eq. (3).

$$\xi_{\mathrm{a}} = 1 - \exp(-f_{\mathrm{T}}(T)t^{n}) \quad (3)$$

$$f_{\mathrm{T}}(T) = a_1\left(\frac{T - a_2}{a_3}\right)^{a_4}\left(\frac{a_5 - T}{a_6}\right)^{a_7} \quad (4)$$

where ξ_{a} is the volume fraction of austenite transformed, $f_{\mathrm{T}}(T)$ a function of temperature T, t the phase transformation time, and the power n a constant. The constant n and the coefficients from a_1 to a_7 in function $f_{\mathrm{T}}(T)$ are determined by using the isothermal phase transformation diagram.

The martensitic phase transformation is modeled by Magee's equation [22], which is given in Eq. (5).

$$\xi_{\mathrm{M}} = 1 - \exp(\psi_1 T + \psi_2) \quad (5)$$

where ξ_{M} is the volume fraction of martensite. ψ_1 and ψ_2 are constants, determined by using the martensitic transformation's starting and finishing temperatures.

During the quenching process of the steel component, both diffusional and martensitic phase transformations may occur simultaneously at different locations of the component. The accuracy of the phase transformation models is very important to the quenching simulation results. The influence of phase transformations on the stress generation during the quenching process is shown later in this paper.

2.3. Stress and deformation analysis

For deformation, the incremental strain is assumed to consist of several terms as shown in Eq. (6).

$$d\varepsilon = d\varepsilon^{\mathrm{e}} + d\varepsilon^{\mathrm{p}} + d\varepsilon^{\mathrm{t}} + d\varepsilon^{\mathrm{tr}} + d\varepsilon^{\mathrm{tp}} \quad (6)$$

where the superscripts e, p, t, tr, and tp represent entities for elastic, plastic, thermal, phase transformations, and transformation plasticity, respectively. Phase transformations and transformation plasticity make the quenching process a highly non-linear problem.

3. Response surface method

The quadratic response surface models are used to describe the relationship between the corresponding properties and the design variables as shown in Eq. (7).

$$f = b_{\mathrm{o}} + \sum_{i=1}^{n} b_i x_i + \sum_{i=1}^{n}\sum_{j=1}^{n} b_{ij} x_i x_j \quad (7)$$

where b_i and $\mathrm{b_{ij}}$ are coefficients, $\mathrm{x_i}$ and $\mathrm{x_j}$ the design variables, and n is the number of design variables. Using the least square method, shown in Eq. (8), the estimates of the regression coefficients are determined. The mixed regression method is used to

improve the fitting accuracy of the response surface models by deleting some unimportant terms.

$$b = (X^{\mathrm{T}}X)^{-1}X^{\mathrm{T}}y \tag{8}$$

where X is the design variable vector and y the response vector of the objective function or constraints.

D-optimality criterion is used to design the experimental points for fitting the response surface models. The number of design points is determined based on the consideration of the number of design variables and the order of the response surface models. The response vectors of the objective function and constraints are calculated using the finite element simulation results at these design points.

4. Example

A disk example is used to demonstrate the optimization scheme introduced in this paper. The material of the component is AISI 4140. Half a cross-section of the axisymmetric component is used for the simulation and optimization. The finite element model includes 496 elements and 563 nodes, as shown in Fig. 2.

4.1. Verification of phase transformation models

The accuracy of the phase transformation models is very important to the quenching simulation results. The latent heat due to phase transformation will influence the cooling history. The volume change due to phase transformation will influence the distortion and residual stress distribution. The accuracy of the phase transformation models are investigated by comparing the hardness distributions predicted by phase transformation models and the Jominy end-quench experimental data.

Two methods can be used to predict the hardness distribution according to the temperature cooling history. The first method is to predict the volume fractions of the different phases using the phase transformation models, which calculates the hardness

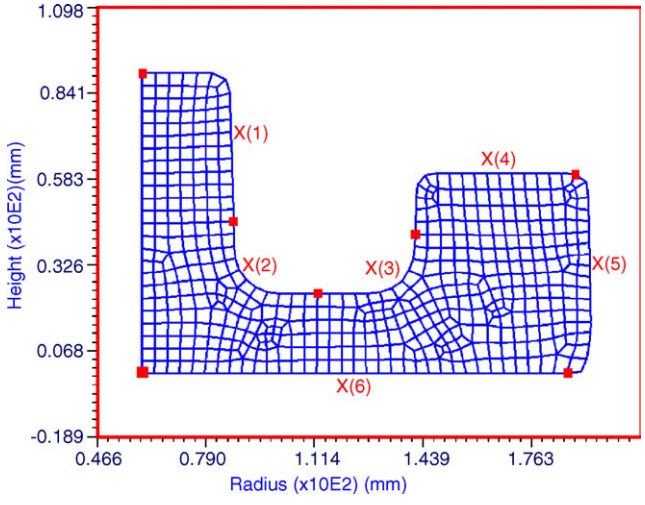

Fig. 2. Design variables of heat transfer coefficients along the surface of the component.

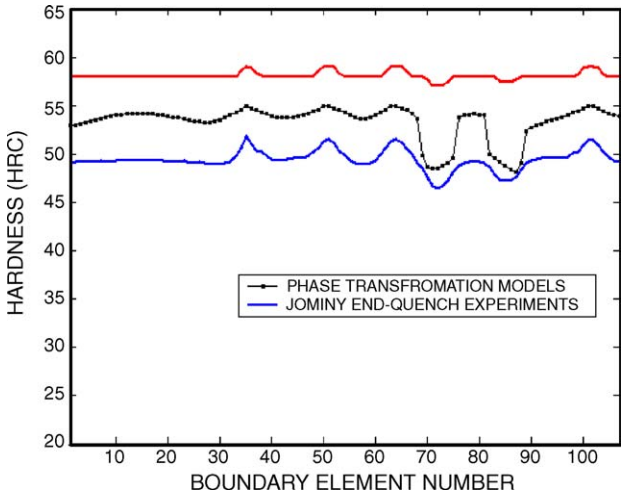

Fig. 3. Comparison of hardness predicted by phase transformation models and Jominy end-quench experimental data.

by the rule of mixtures. The second method is to calculate the hardness according to the cooling rate by using the Jominy end-quench experimental data. The second method is well accepted, and the Jominy end-quench experimental data is available in the ASM Metals Handbook [23]. Therefore, the accuracy of the phase transformation models can be investigated by comparing the hardness predicted by these two methods. Using the example shown in Fig. 2, the hardness values are calculated by both methods. Fig. 3 shows the comparison results. The X-coordinate is the element number along the surface of the component. The solid lines are the upper and lower hardness bounds predicted by the Jominy end-quench experimental data. The middle line is the hardness calculated by the phase transformation models. The hardness, predicted by the phase transformation models, is located between the upper and lower hardness bounds predicted by the Jominy end-quench experimental data, which means the phase transformation models are acceptable. During the quenching process, the phase transformations have significant influence on the distortion and residual stress distribution, which is shown later in this paper. Therefore, the phase transformation models are used to calculate the hardness after being verified.

4.2. Modeling of heat transfer coefficient

The design of the heat transfer coefficient is very important to the quality of the quenching product. Different mathematical models can be used to describe the heat transfer coefficient. Based on the irregular surface geometry of the component, a uniform heat transfer coefficient will cause various heat flux values along the surface of the component. The heat flux and cooling rate will be less at the convex corners than at the concave corners if the same heat transfer coefficient is used. The modeling of the heat transfer coefficient along the surface of the component should be based on the geometry of the component. In this paper, the surface of the component is divided into six regions, as shown in Fig. 2, and different heat transfer coefficients are imposed on each region. The heat transfer coefficient is constant in time and temperature. The values of the heat transfer

coefficient on different regions are represented by $X(1)$, $X(2)$, ..., $X(6)$. The six heat transfer coefficients are used as design variables to optimize the gas quenching process.

4.3. Calculation of functional properties

Distortion caused by quenching will result in increased cost due to post-manufacturing processes, such as grinding and hot rectification. The objective function in this problem is to minimize the distortion of the as-quenched component. The distortion in this paper is defined as the shape difference between the desired component and the final shape after quenching with compensation for volume change. A schematic plot of distortion is shown in Fig. 4. The desired shape and final shape are drawn in dashed line and solid line, respectively. The areas *A*, *B*, *C* and *D* represent the shape differences between the desired and final shapes. The distortion is calculated as the addition of the absolute values of the four areas. The boundary nodal coordinates of the desired and final shapes are used to calculate the area difference *A*, *B*, *C* and *D* by the Green theorem. The residual stress and surface hardness distribution have significant influences on the service quality of the quenched product. The first constraint is imposed on the maximum principal residual stress, which can be extracted from the simulation results. Two constraints are imposed on the average surface hardness and the standard deviation of the surface hardness to improve the service quality of the component.

The average surface hardness and the standard deviation of the surface hardness can be calculated according to the hardness of all surface elements. Investigation on the fitting accuracy found that the response surface model of the surface hardness standard deviation has a large approximation error, which is not suitable for use in optimization. In this problem, the response surfaces of hardness at six surface control points are

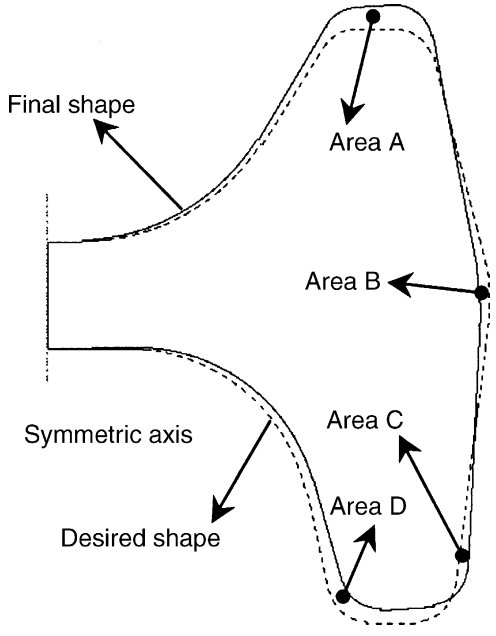

Fig. 4. Definition of distortion.

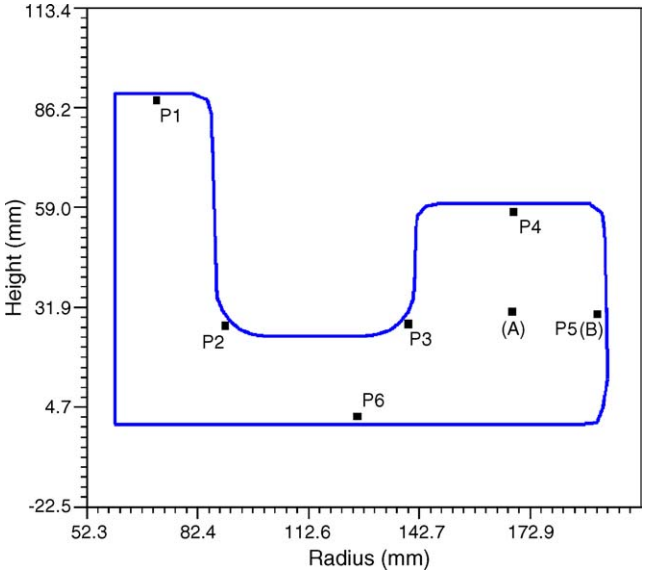

Fig. 5. Six control points on the surface of the component.

approximated individually in terms of heat transfer coefficient design variables. These six points are shown in Fig. 5 as P1, P2, ..., P6. The analysis of variance shows that the response surfaces of hardness at these six points have good modeling accuracy. The average surface hardness and standard deviation of the surface hardness are calculated by using the closed-form response surface models. Usually, the response surfaces of the average surface hardness and the standard deviation of the surface hardness do not have good fitting accuracy. By using Eqs. (9) and (10) instead of fitting their response surface models directly, the poor fitting accuracy problem can be avoided.

The average surface hardness is calculated by using Eq. (9).

$$\bar{H} = \frac{\sum_{i=1}^{6} H_i}{6} \tag{9}$$

where $\bar{H}$ is the average surface hardness of these six points; H_i the hardness at the *I*-th surface point.

The standard deviation of the surface hardness is calculated by Eq. (10).

$$H_{\mathrm{d}} = \sqrt{\frac{\sum_{i=1}^{6} (H_i - \bar{H})^2}{5}} \tag{10}$$

where H_{d} is the standard deviation of the hardness at these six control points.

Two points are used as observable points to check the stress variation during the gas quenching process. Point B is at the surface of the component, and point A is an internal point, as shown in Fig. 5.

The contributions of the phase transformations and the thermal gradient on the stress generation can be seen from Fig. 6. At the beginning of the quenching process, there are no phase transformations, and the thermal stress is the only contribution. At this time period, the surface point has a tensile stress and the internal point has a compressive stress. After about 40 s

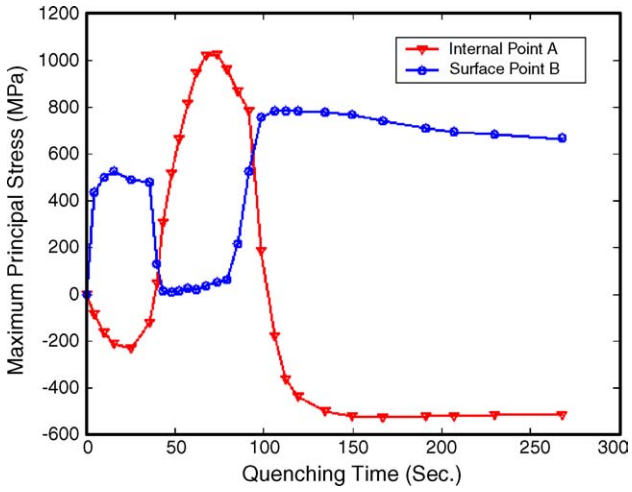

Fig. 6. Stress variation during the quenching process.

of quenching, the stress at the surface point changes from tensile to compressive stress. On the other hand, the stress at the internal point converts from compressive to tensile stress. This phenomenon comes from the volume increase due to the martensitic phase transformation in the surface of the component. With the increase of the quenching time, the martensitic phase transformation in the surface of the component finished, and the martensitic and diffusional phase transformations in the internal part of the component started. Due to the volume increase of the martensitic and diffusional phase transformations, the stress at the internal point of the component converts from tensile to compressive, and vice versa at the surface point. Phase transformation is a very important issue during the quenching process, especially for the residual stresses and distortion prediction.

For different shape and size of component, the phase transformation sequences during the quenching process may be different. Therefore, the stress generation history may also be different from the example shown in Fig. 6. After the quenching process, presence of tensile stresses on the surface of the component is not preferred, because it could reduce the fatigue strength and life of the component. For a quenched steel component, tempering treatment is needed to reduce the residual stresses, also increase the toughness of the component by transferring the as-quenched martensite (body centered tetragonal structure) to tempered martensite (body centered cubic structure).

4.4. Optimization model

Six heat transfer coefficients are used as design variables to optimize the gas quenching process. The design space of this example is listed in Table 1. The determination of the design space is based on two considerations. One is that the required average surface hardness can be obtained in this design space. The other is that it should be possible to implement this heat transfer coefficient in a manufacturing facility. It has been shown that high pressure helium quenching has the capacity to replace quenching oils, even faster quenching oils, when high pressure, 20 bar and above are used [24].

Table 1
Design space

Design variables	Lower bound	Middle point	Upper bound
Coded value	−1	0	+1
$X(1)$ (kW/m^2 K)	1.0	1.5	2.0
$X(2)$ (kW/m^2 K)	1.0	1.5	2.0
$X(3)$ (kW/m^2 K)	1.0	1.5	2.0
$X(4)$ (kW/m^2 K)	1.0	1.5	2.0
$X(5)$ (kW/m^2 K)	1.0	1.5	2.0
$X(6)$ (kW/m^2 K)	1.0	1.5	2.0

The normalized optimization model is listed as follows:
Minimize:

$$\text{obj.} = \frac{\text{distortion}}{50.00} \tag{11}$$

Subject to:

$$G(1) = \frac{\sigma_{\text{mp}}}{1000.0} - 1.0 \le 0 \tag{12}$$

$$G(2) = 1.0 - \frac{\bar{H}}{50.0} \le 0 \tag{13}$$

$$G(3) = \frac{H_{\text{d}}}{1.0} - 1.0 \le 0 \tag{14}$$

where σ_{mp} is the maximum principal residual stress; $\bar{H}$ and H_{d} are the average surface hardness and the standard deviation of the surface hardness, respectively.

Response surface method is used to build the relations between the functional properties and the design variables. Fifty design of experimental points identified by the D-optimality criterion are used to build the closed-form equations. For distortion and the maximum residual principal stress, the response surface models are built directly according to the simulation results. Response surface models of hardness at the six surface points, shown in Fig. 4, are fitted separately. Then using Eqs. (9) and (10), the average surface hardness and the standard deviation of the surface hardness are calculated.

5. Results and discussions

The optimization results are shown in Table 2, together with a reference design. The reference design point locates at the center of the design space. At the optimum design point, four design variables, $X(2)$, $X(3)$, $X(4)$ and $X(5)$ are located at or close to the upper bound. The objective function is to minimize the distortion of the as-quenched component. Three constraints are imposed on the maximum principal residual stress, average surface hardness, and the standard deviation of the surface hardness. After optimization, all constraints are satisfied. As four design variables are located at the upper bound, it is possible to minimize the distortion further by increasing the upper bound of the design variable. Based on this consideration, the upper bound of the design space is increased to 2.5 kW/m^2 K instead of the initial value of 2.0 kW/m^2 K. Using the initial 50 trial points, the fitting accuracy of the response surface models is damaged because the upper bound of the design space is increased. By adding

Table 2
Comparison of optimum design with reference design

	Reference design	Optimum design
$X(1)$ (kW/m^2 K)	1.5	1.42
$X(2)$ (kW/m^2 K)	1.5	1.96
$X(3)$ (kW/m^2 K)	1.5	1.99
$X(4)$ (kW/m^2 K)	1.5	2.00
$X(5)$ (kW/m^2 K)	1.5	2.00
$X(6)$ (kW/m^2 K)	1.5	1.58
Objective	1.5926	0.70
$G(1)$	−0.0050	−0.024
$G(2)$	−0.0022	−0.080
$G(3)$	4.89	−0.58
Distortion (mm^2)	79.63	35.21
σ_{mp} (MPa)	995.02	975.96
$\bar{H}$ (HRC)	50.11	54.01
H_d (HRC)	5.89	0.42

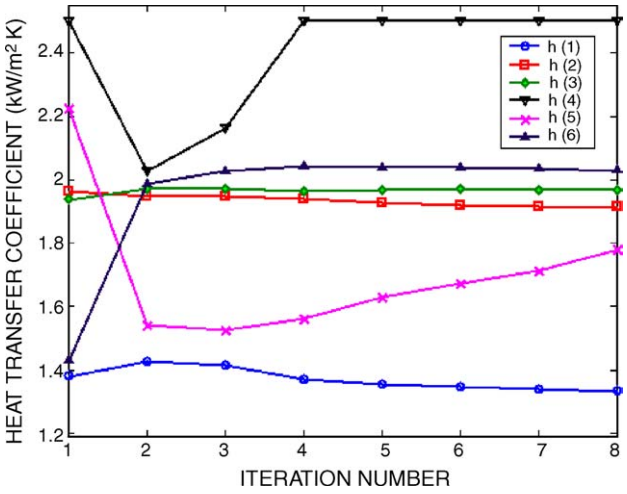

Fig. 8. Changes of heat transfer coefficient with the number of iterations.

the intermediate optimum design points to the initial trial point set, new response surface models are built with improved fitting accuracy. This iteration is continued until the functional properties predicted by the response surface models match the finite element simulation results at the optimum design point. Fig. 7 shows the change of distortion with the number of iterations. At the first iteration, the distortion predicted by two methods has a significant difference. This is because the upper bound of the design space during optimization is increased, however, the design space of the trial point set remains same. With the number of iterations increasing, the difference of distortion predicted by two methods is reduced. At the fourth iteration, the distortion predicted by the finite element simulation has a minimum value of 29.19. And the distortion does not have significant changes with more iterations. The distortion predicted by two methods matches at the eighth iteration.

The changes of the design variable values with the number of iterations are shown in Fig. 8. The fourth iteration is taken as the final optimum design because of its minimum distortion value with the satisfied constraints. After optimization, the fourth design variable, $X(4)$ is located at the upper bound. Investigation shows that $X(4)$ does not have significant influence on the distortion and residual stresses. According to the influences of the heat transfer coefficient on the functional hardness properties, higher heat transfer coefficient is always preferred. This is the reason why $X(4)$ reaches the upper bound. Table 3 shows the improved optimum design. According to [24], the heat transfer coefficient value can reach 2.5 kW/m^2 K with the furnace pressure over 40 bar, and the fluid speed of 15 m/s. There was no reference found in the literature about the high-pressure gas-quenching furnace with the flexibility of nozzle design. However, because the advantages of the gas quenching, and the industry demands [18], the high-pressure gas quenching equipment with the flexibility of heat transfer coefficient control would be developed soon and used in industry.

The distortion of the improved optimum design is reduced comparing with the initial design. The other functional properties do not have significant changes.

Comparing with the reference design, the standard deviation of the surface hardness is reduced significantly after optimization. The reduction of the standard deviation means the surface

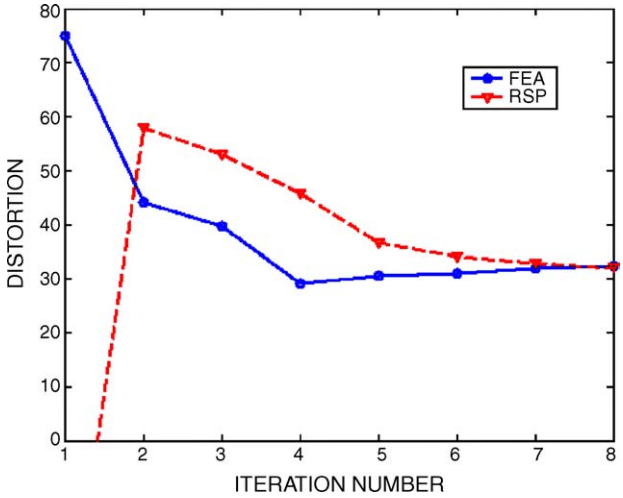

Fig. 7. Change of distortion with the number of iterations.

Table 3
Comparison of the initial and improved optimum designs

	Initial optimum design	Improved optimum design
$X(1)$ (kW/m^2 K)	1.42	1.37
$X(2)$ (kW/m^2 K)	1.96	1.94
$X(3)$ (kW/m^2 K)	1.99	1.96
$X(4)$ (kW/m^2 K)	2.00	2.5
$X(5)$ (kW/m^2 K)	2.00	1.56
$X(6)$ (kW/m^2 K)	1.58	2.04
Objective	0.70	0.58
$G(1)$	−0.024	−0.039
$G(2)$	−0.080	−0.081
$G(3)$	−0.58	−0.57
Distortion (mm^2)	35.21	29.19
σ_{mp} (MPa)	975.96	960.69
$\bar{H}$ (HRC)	54.01	54.05
H_d (HRC)	0.42	0.43

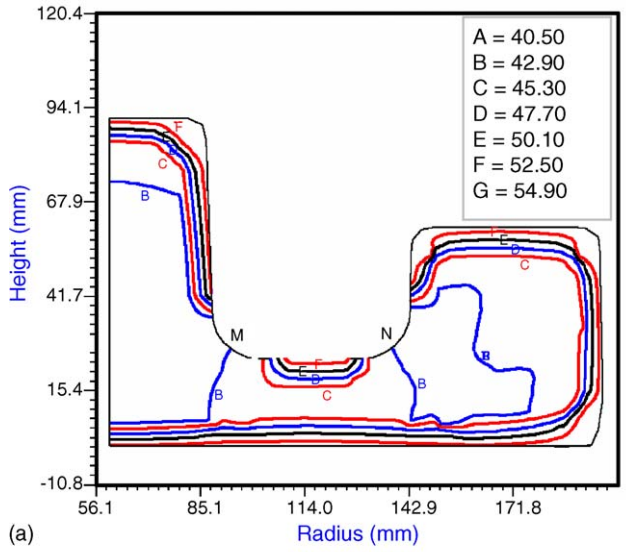

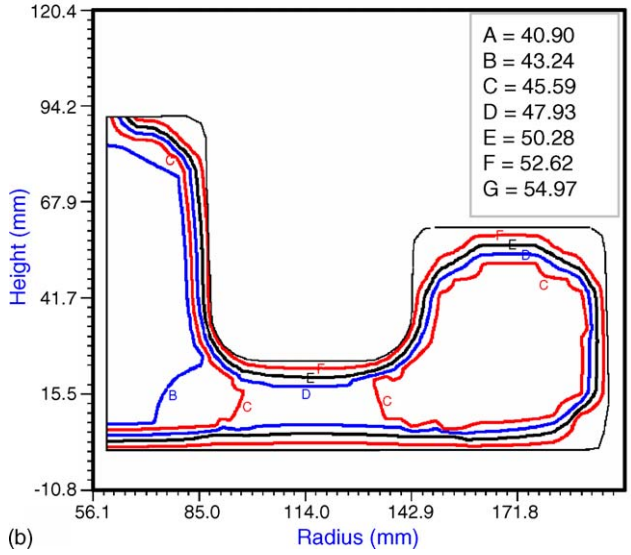

Fig. 9. Hardness distributions (HRC): (a) reference design; (b) optimum design.

hardness distribution is more uniform after optimization. This can also be seen by comparing the hardness distribution contours of both the reference and optimum designs, as shown in Fig. 9.

Fig. 9(a) is the hardness distribution of the reference design. The hardness values at the two convex corners, M and N, are lower. This is because the heat flux at these two corners is lower if a constant heat transfer coefficient is imposed along the surface of the component. Design variables of the heat transfer coefficient should be chosen wherever the geometry of component surface changes. In this example, the design variables $X(2)$ and $X(3)$ are imposed on the two convex corners M and N. The hardness distribution of the optimum design is shown in Fig. 9(b).

After optimization, the average surface hardness is 54 HRC instead of 50 HRC, which makes the constraint on the average surface hardness active. This constraint, however, is necessary to obtain higher average surface hardness value. Without

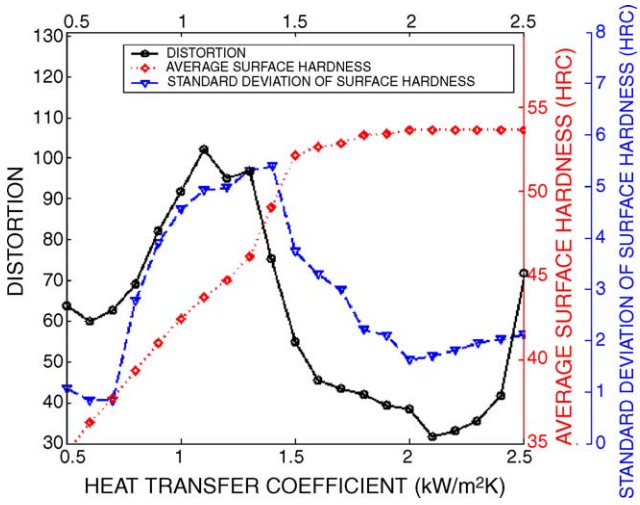

Fig. 10. Heat transfer coefficient influence on functional properties.

using this constraint, the average surface hardness value can be very low for the pursuit of less distortion and standard deviation of surface hardness, which can be seen from Fig. 10. In Fig. 10, the heat transfer coefficient along the surface of the component is a constant. With the increase of the heat transfer coefficient, the distortion and the standard deviation of the surface hardness increase first, then decrease. Therefore, without the constraint on the average surface hardness, the optimum design point can locate at both the left and right of the peaks. Even though Fig. 10 is obtained based on the assumption of a constant heat transfer coefficient along the surface of the component, it can still explain the reason why the constraint on the average surface hardness is not active to reduce the objective function.

6. Conclusions

The heat transfer coefficient along the surface of the component is designed to optimize the gas quenching process. The response surface method provides an effective way to optimize the heat transfer coefficient when the sensitivity information is not available. The hardness at six surface points are used to build the response surfaces in terms of the heat transfer coefficient variables. Then the average surface hardness and the standard deviation of the surface hardness are calculated based on these individual response surfaces. This scheme can avoid the high fitting error problem of the response surface model of the surface hardness standard deviation. After optimization, the distortion is minimized, and the surface hardness distribution is much more uniform.

Acknowledgements

This project was funded by the NIST ATP OSURF # 64921-55-00. The first author's Graduate Research Assistantship was supported by the Dayton Area Graduate Study Institute (DAGSI).

References

[1] R. Holoboff, B.L. Hote, R. Speri, O. Delcourt, Gas quenching with helium, Adv. Mater. Process. 143 (2) (1993) 23–26.

[2] T. Lübben, F.T. Hoffmann, P. Mayr, C. Laumen, The uniformity of cooling in high-pressure gas quenching, Heat Treat. Metals 27 (3) (2000) 57–61.

[3] F.T. Hoffmann, T. Lübben, P. Mayr, Innovations in quenching systems and equipment: current status and future development, Heat Treat. Metals 26 (3) (1999) 63–67.

[4] G.C. Carter, Optimizing gas quenching, Adv. Mater. Process. 149 (2) (1996) 79–82.

[5] J.R. Davis, et al. (Eds.), ASM Handbook, vol. 4, American Society for Metals, Metals Park, OH, 1991, pp. 638–656.

[6] T.C. Tszeng, W.T. Wu, J.P. Tang, Prediction of distortion during heat treating and machining processes, in: Proceedings of the 16th ASM Heat Treating Society Conference and Exposition, Cincinnati, OH, 1998, pp. 9–15.

[7] T. Inoue, K. Arimoto, Development and implementation of CAE system HEARTS for heat treatment simulation based on metallo-thermo-mechanics, J. Mater. Eng. Perform. 6 (1) (1997) 51–60.

[8] Y.H. Guan, T.L. Chen, H.G. Wang, J.T. Zhang, The prediction of the mechanical properties of metal during laser quenching, J. Mater. Process. Technol. 63 (1997) 614–617.

[9] D.F. Watt, L. Coon, M. Bibby, J. Goldak, C. Henwood, An algorithm for modeling microstructural development in weld heat-affected zones reaction kinetic, Acta Metall. 36 (1988) 3029–3035.

[10] R.A. Wallis, N.M. Bhathena, P.R. Bhowal, E.L. Raymond, Application of process modeling to heat treatment of superalloys, Indust. Heat. 55 (1988) 525–534.

[11] R.A. Wallis, P.R. Bhowal, N.M. Bhathena, E.L. Raymond, Modeling the heat treatment of superalloy forgings, J. Metals 41 (1989) 35–37.

[12] P.J. Röhl, S.K. Srivatsa, A comprehensive approach to engine IPPD, AIAA-97-1113 (1997) 1250–1257.

[13] M. Batista, F. Kosel, Sensitivity analysis of heat treatment of steel, AIAA-96-4152 (1996) 1452–1460.

[14] R. Karthikeyan, P.R.L. Narayanan, R.S. Naagarazan, Heat treatment optimization for tensile properties of Al/SiCp metal matrix composites using design of experiments, Process. Fabricat. Adv. Mater. 5 (1998) 703–711.

[15] A. Saigal, G. Leisk, Taguchi analysis of heat treatment variables on the mechanical behavior of alumina/aluminum metal matrix composites, Composit. Eng. 5 (2) (1995) 129–142.

[16] Scientific Forming Technologies Corporation, DEFORM Users Manual, 5038 Reed Road, Columbus, OH 43220, 1999.

[17] Vanderplaats Research and Development Inc., Design Optimization Tools (DOT) Users Manual, 1767 South 8th Street Suite 210, Colorado Springs, CO 80906, 1995.

[18] R.N. Dixon, Meeting Industry Demands for Rapid Gas Quenching Systems for Vacuum Heat Treating Equipment, in: Proceedings of the 16th ASM Heat Treating Society Conference and Exposition, 19–21 March 1996, Cincinnati, Ohio, pp. 187–196.

[19] B.H. Morales, J.K. Brimacombe, E.B. Hawbolt, S.M. Gupta, Determination of quench heat transfer coefficients using inverse techniques, in: Proceedings of the First International Conference on Quenching and Control of Distortion, September 1992, Chicago, Illinois, pp. 155–164.

[20] Z. Li, R.V. Grandhi, Optimal heat treatment design in manufacturing, in: The Seventh International Conference on Numerical Methods in Industrial Forming Processes, 18–21 June 2001, Toyohashi, Japan.

[21] W.A. Johnson, F.R. Mehl, Reaction kinetics in processes of nucleation and growth, Trans. AIME 135 (1939) 416–425.

[22] C.L. Magee, Phase transformations: papers presented at a seminar of the American Society for Metals, American Society for Metals, Metals Park, OH, 1968, pp. 115–154.

[23] J.R. Davis, et al. (Eds.), ASM Handbook, vol. 1, American Society for Metals, Metals Park, OH, 1991, pp. 464–484.

[24] S.J. Midea, T. Holm, et al., High pressure gas quenching—technical and economical considerations, in: Proceedings of the Second International Conference on Quenching and Control of Distortion, 4–7 November 1996, Cleveland, Ohio, pp. 157–163.